Radiology

Removal of Antiscatter Grids for Spinal Digital Subtraction Angiography: Dose Reduction without Loss of Diagnostic Value

*Emanuele Orrù, MD** • *Amgad El Mekabaty, MD** • *Diego San Millan, MD* • *Monica S. Pearl, MD* • *Philippe Gailloud, MD*

From the Division of Interventional Neuroradiology, The Johns Hopkins Hospital, 1800 E Orleans St, Baltimore, MD 21287. Received August 9, 2019; revision requested September 30; revision received December 9; accepted December 30. **Address correspondence to** P.G. (e-mail: *phg@jhmi.edu*).

Supported by the National Center for Research Resources and National Center for Advancing Translational Sciences of the National Institutes of Health (1UL1TR001079).

* E.O. and A.E.M. contributed equally to this work.

Conflicts of interest are listed at the end of this article.

Radiology 2020; 295:390–396 • https://doi.org/10.1148/radiol.2020191786 • Content code: NR

Background: Spinal digital subtraction angiography (DSA) exposes patients and operators to substantial amounts of radiation. Antiscatter grid (ASG) removal is used to decrease radiation exposure but may reduce image quality.

Purpose: To determine whether ASG removal during spinal DSA in adults reduces radiation dose while maintaining diagnostic image quality and whether dose reduction is related to body mass index (BMI).

Materials and Methods: This Health Insurance Portability and Accountability Act–compliant prospective study included adults undergoing spinal DSA between January and December 2016. Each procedure included an additional angiographic acquisition performed twice, once with and once without ASG, either documenting the artery of Adamkiewicz (no pathology group) or the condition leading to the procedure (pathology group). Dose differences between study acquisitions and the influence of BMI were evaluated via paired *t* test. Two neurointerventionalists blinded to acquisition protocols were asked to independently evaluate a sample of 40 study acquisitions (20 with ASG, 20 without ASG) from 20 randomly selected participants to *(a)* rate image quality, *(b)* categorize findings, and *(c)* determine whether images had been obtained with or without ASG. Percentage agreement on image quality, findings categorization, and ability to correctly identify the acquisition protocol was calculated for both readers.

Results: Fifty-three participants (mean age ± standard deviation, 51 years ± 15.2; 32 men) were evaluated. ASG removal reduced the mean dose per acquisition by approximately 33% (mean dose-area product and air kerma decreased from 202 to 135.6 μGy/m^2 and from 35.3 to 24 mGy, respectively; $P < .001$) independently of BMI ($P = .3$). Both readers evaluated all images (40 of 40) as being of diagnostic quality and correctly categorized findings in 19 of 20 (95%) cases. Overall percentage agreement for correct protocol identification was 60% (12 of 20) for grid-in and 45% (nine of 20) for grid-out images.

Conclusion: Antiscatter grid removal during spinal digital subtraction angiography decreased participants' radiation exposure while preserving diagnostic image quality.

Spinal digital subtraction angiography (DSA) is the reference imaging method used to investigate the spinal vasculature (1–5). Complete spinal DSA includes the selective study of each pair of intersegmental arteries of aortic origin (most often T3–L3), the subclavian artery and its branches (including the vertebral and supreme intercostal arteries), the carotid arteries, and the pelvic circulation (median and lateral sacral arteries). This large number of injections can require potentially long fluoroscopic times; thus, it is important to minimize radiation exposure to the patient and angiography team. Modern angiography suites are equipped with removable antiscatter grids (ASGs) made of parallel lead strips. ASGs filter the scattered x-rays produced by the passage of the beam though the patient's tissues, allowing only the primary x-rays to reach the detector and form the radiographic image. By optimizing the signal-to-noise ratio, ASGs improve image quality. However, because only a fraction of the generated x-rays participate in the formation of the radiographic image, the use of ASGs is associated with an increase in radiation exposure.

ASG removal is a well-known but rarely investigated and scarcely applied radioprotection technique; its advantages have been mostly studied in the pediatric population and in the interventional cardiology field, with only a few mentions of cerebral angiography and temporal bone imaging (6–15). We sought to investigate ASG removal in the adult population undergoing spinal DSA because of the substantial amount of radiation associated with the procedure.

The purpose of this prospective study was to test the hypothesis that ASG removal significantly reduced the dose in spinal DSA while maintaining diagnostic image quality and to evaluate whether dose reduction was related to the participants' body mass index (BMI).

Abbreviations

ASG = antiscatter grid, BMI = body mass index, DAP = dose-area product, DSA = digital subtraction angiography, $K_{a,r}$ = reference air kerma

Summary

Removal of antiscatter grids during spinal angiography reduces radiation exposure to patients and operators while maintaining acceptable diagnostic image quality; this dose-reduction technique may be applied to any fluoroscopy-based thoracic or abdominal procedure.

Key Results

- Antiscatter grid removal during spinal angiography reduced radiation dose by approximately 30% independently of the participant's body mass index ($P < .001$).
- Despite significant dose reduction by approximately 33%, the diagnostic quality of images used to investigate minute spinal vascular structures was maintained.

Materials and Methods

The institutional review board approved this prospective study, which complied with the Health Insurance Portability and Accountability Act. All participants signed a consent form explaining the study and were given the option to withdraw participation at any time. The obtained data were exclusively used for this study, and there is no overlap with any other past or future publication.

Study Design

The study participants underwent diagnostic spinal DSA. Body habitus determined whether angiography was performed in its entirety with or without ASGs. Participants with a BMI of 40 kg/m^2 or greater underwent the entire procedure with the ASG, while those with a BMI of less than 30 kg/m^2 underwent the procedure without it; in those with a BMI of 30–39 kg/m^2, the operators made the decision on an individual basis. After completion of the diagnostic procedure, an intersegmental artery was selected for an additional acquisition with or without ASGs, depending on how the entire examination had been performed. In case of negative DSA findings (no abnormality group), the intersegmental vessel providing the artery of Adamkiewicz was selected, whereas in cases with a vascular abnormality (abnormality group), the targeted artery was the main feeder to the lesion. The artery of Adamkiewicz was chosen because it is the most important and constantly present radiculomedullary feeder, and its visualization is essential for spinal DSA to be considered diagnostic.

Study Participants

Participants were men and women undergoing spinal DSA at our institution between January and December 2016. Pediatric patients were excluded. Test acquisitions were not performed in eight participants who were tired or uncomfortable at the end of the procedure. Four participants were excluded early in the study because of the inadvertent application of a different copper filtration protocol between test acquisitions (Fig 1).

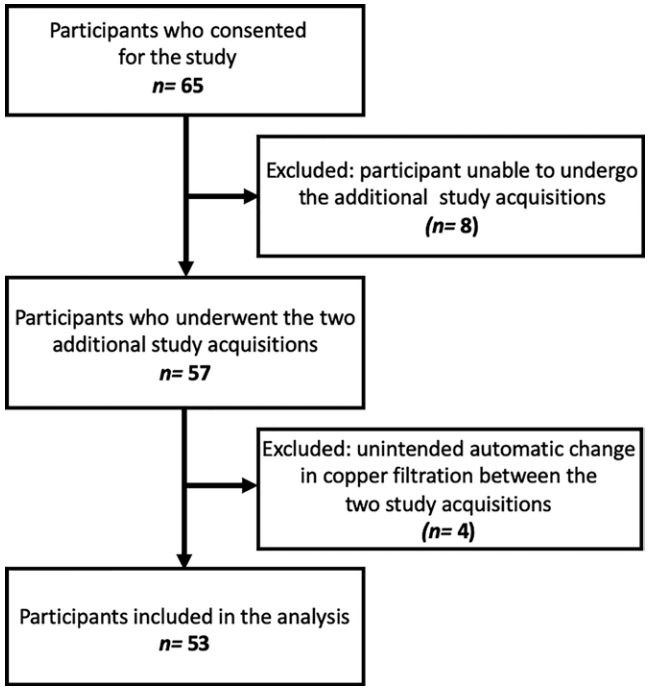

Figure 1: Participant flowchart.

Image Acquisition

Spinal DSA was performed in a biplanar neuroangiography suite with a total of 76 102-cm flat-panel detectors (Artis Zee; Siemens Healthineers, Erlangen, Germany). Two fixed-length protocols were designed for the study: a 10-second variable frame rate protocol with a total of 11 images and a 16-second variable frame rate protocol with a total of 14 images. The need to assess the venous phase determined the chosen protocol. Test acquisitions were obtained in the posteroanterior projection with input field sizes of 32, 42, or 48 cm. An angiographer (P.G.) with 25 years of experience in spinal vascular procedures performed all the contrast material injections by hand using the same volume of contrast material at the same concentration: 3 mL of a solution of 75% iohexol (Omnipaque 300; GE Healthcare, Little Chalfont, United Kingdom) and 25% saline. Parameters such as patient-source and patient-detector distances, input field size, automatic exposure control, focal spot, and copper filtration were kept identical for both test acquisitions. Values for reference air kerma ($K_{a,r}$, in milligrays) and dose-area product (DAP, in micrograys per square meter) were automatically recorded by the angiography system.

Image Quality Evaluation

The evaluation was based on the review of 40 images (ie, one image from each test acquisition) in 20 randomly selected participants either documenting the artery of Adamkiewicz or a vascular abnormality (10 cases each). Images were chosen by the senior author (P.G.) and documented the important finding at the time of maximum contrast opacification. The images were randomly organized in a 40-slide electronic document and were assessed separately in a blinded random manner by two clinically active senior fellowship–trained

neurointerventionalists (M.S.P., D.S.M.; 9 and 23 years of experience in spinal angiographic procedures, respectively) who had no information about the participants' population and were not involved in protocol design or image acquisition. The two readers were asked to fill, independently and in a single session, an evaluation form with a three-point quality scale similar to forms previously used for subjective image assessments (good, moderate, or poor based on image degradation by noise) (16). Good-quality images were considered to be of excellent diagnostic quality, moderate-quality images were, in the readers' opinion, still of diagnostic value but were more degraded by noise. Images of poor quality were considered unacceptable for clinical evaluation and were ultimately nondiagnostic. The readers were asked to assign images to one of three categories—no abnormality, vascular malformation, or tumor—and to determine whether they had been obtained with or without ASGs.

Statistical Analysis

The $K_{a,r}$ and DAP per image and the relative ratios between test acquisitions (with or without ASGs) were used to calculate the mean and standard deviations of dose reduction rates. A paired *t* test was applied to evaluate the change in $K_{a,r}$ and DAP between the two test acquisitions. Participants were stratified by BMI (as a categorical variable, low BMI [≤25 kg/m^2] vs high BMI [>25 kg/m^2]) to determine whether dose reduction depended on BMI status. Correlation between dose reduction and both ASG removal and BMI was analyzed with a Spearman test. Analyses were performed by using Stata, version 15, software (Stata, College Station, Tex). $P < .05$ was considered representative of statistical significance.

The percentage agreement was calculated for image quality assessment, diagnosis, and protocol recognition for each reviewer to determine whether assessment differed between images obtained with or without ASGs. Interrater percentage agreement was also calculated for the previously mentioned parameters for images obtained with or without ASGs. We considered a percentage agreement level between readers of 80% or greater to be clinically acceptable.

Results

Study Participants

Data acquired in 53 study participants (32 men [60%]) were included in the final analysis. Forty-three of 53 (81%) underwent diagnostic spinal DSA, and 10 of 53 (19%) underwent therapeutic procedures. The mean age was 51 years ± 15 (standard deviation) (range, 20–83 years). Mean BMI was 27.3 kg/m^2 ± 5.7 (range, 16.4–40.7 kg/m^2). The main indication for spinal angiography was progressive myelopathy, occurring in 31 of 53 (58%) participants. Participants' demographic characteristics and procedural indications are listed in Table 1.

Table 1: Characteristics of Participants Undergoing Spinal Angiography

Parameter	Value
Sex	
Men	32 (60)
Women	21 (40)
Age (y)	
All participants	51 ± 15.2 (20–83)
Men	50 ± 17.3 (20–83)
Women	53 ± 11.2 (32–69)
BMI	
All participants	27 ± 5.7 (16.4–40.7)
Men	26 ± 4.6 (16.4–35)
Women	29 ± 7.0 (19.2–40.7)
Low BMI (*n* = 20)	21 ± 1.6 (16.4–24)
High BMI (*n* = 33)	31 ± 4.2 (25.2–40.7)
Type of angiography	
Diagnostic	43 (81)
Interventional	10 (19)
Sedation or anesthesia	
Conscious sedation	40 (75)
General anesthesia	13 (25)
Indication for spinal angiography	
Progressive myelopathy	31 (58)
Tumor (diagnostic or preoperative embolization)	12 (23)
Known spinal vascular malformations	5 (9)
Spinal cord hemorrhage	2 (4)
Other	3 (6)

Note.—Unless otherwise specified, data are numbers of participants (*n* = 53) with percentages in parentheses or means ± standard deviation with ranges in parentheses. BMI = body mass index. Low BMI, ≤25 kg/m^2; high BMI, >25 kg/m^2.

Dose Study

The mean $K_{a,r}$ was 35.3 mGy ± 13.7 with ASGs and 24.0 mGy ± 10.6 without ASGs. The mean DAP was 202.0 μGy/m^2 ± 100.2 with ASGs and 135.6 μGy/m^2 ± 68.5 without ASGs. ASG removal led to a dose reduction of 33% in $K_{a,r}$ ($P < .001$) and 33% in DAP ($P < .001$). The dose reduction remained significant when $K_{a,r}$ and DAP reduction was compared between participants with low and high BMI; there was no significant difference in the degree of dose reduction between the two groups (Spearman correlation = 0.18 [$P = .32$] for $K_{a,r}$ and 0.37 [$P = .06$] for DAP). Figure 2 depicts the mechanism at the basis of dose reduction in angiography with and without ASG. Detailed changes in radiation dose after removal of the ASGs are summarized in Table 2.

Image Quality Assessment

All images obtained with ASGs were rated as good by reader 1 (20 of 20 cases [100%]). These images were rated as good in 19 of 20 cases (95%) by reader 2; one of 20 cases (5%) was rated as moderate. The images obtained without ASGs were rated as good in 95% of cases (19 of 20) by reader 1 and in 75% of cases (15 of 20) by reader 2. One was rated as moderate (5% [one of 20]) by reader 1, and five were rated as moderate (25% [five of 20]) by reader 2. All images were of diagnostic quality; none were rated poor by either reader.

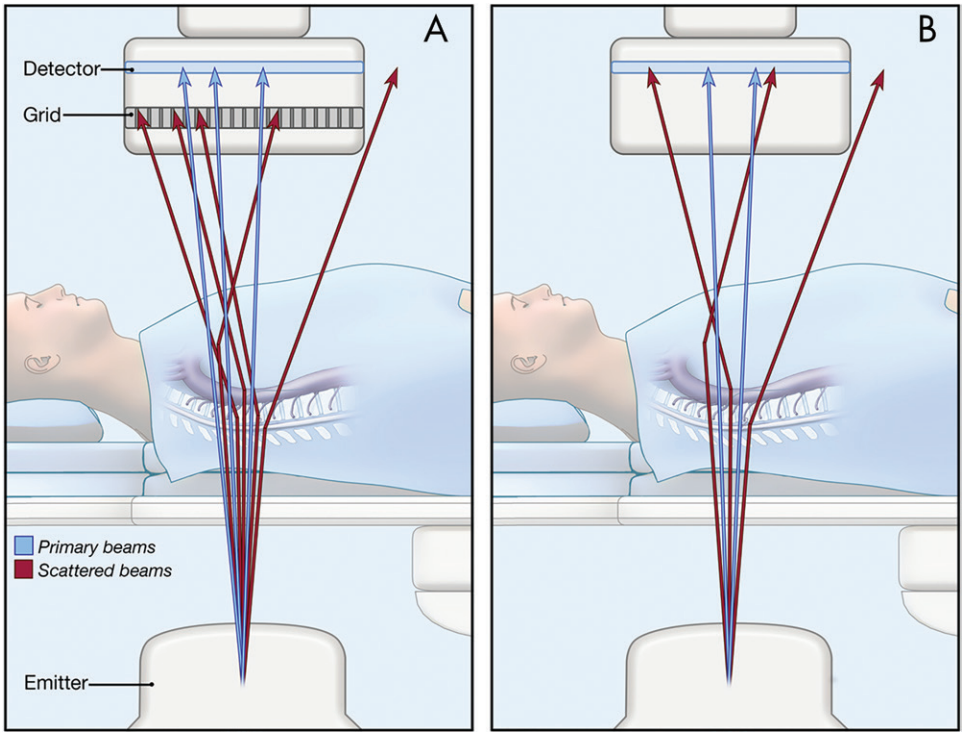

Figure 2: Illustration shows angiography with or without antiscatter grids. *A*, With the grids in place, only primary x-rays reach the detector. The angiographic image is sharper, but its production requires more x-rays. *B*, Without the grids, both primary and scattered x-rays reach the detector. The image loses some sharpness, but its formation requires a lower radiation dose. (Illustration by Lydia Gregg, MA, Baltimore, Md.)

The agreement in quality assessment between images acquired with ASG and those acquired without it was 95% (38 of 40) for reader 1 and 80% (32 of 40) for reader 2. The overall agreement between both readers for the quality of images was 95% (19 of 20) for those with ASG and 80% (16 of 20) for those without it; therefore, agreement was considered better than acceptable for both image types.

Key Finding Assessment

The readers correctly classified the key finding in 95% (19 of 20) of images obtained with or without ASGs. Both readers erroneously classified the key finding in one participant (different case for each reader). Reader 1 classified one "no abnormality" image as "vascular malformation" and reader 2 classified one "tumor" image as "no abnormality." One misclassified image was obtained with ASGs, and one was obtained without them. The overall agreement between both readers for correct identification of key findings in images obtained with or without ASGs was 90% (18 of 20).

Grid Status Identification

Reader 1 correctly identified the grid status (image obtained with or without ASGs) in 60% (24 of 40) of cases; reader 2 did so in 58% (23 of 40) of cases. The overall percentage agreement between readers when they evaluated images obtained with ASGs was 60% (12 of 20) but fell to 45% (nine of 20) when the analysis was restricted to the images in which the protocol was correctly identified. For images obtained without ASGs, the overall percentage agreement and the agreement restricted to images where the protocol was correctly identified were 45% (nine of 20) and 25% (five of 20), respectively. Representative examples of test acquisitions are shown in Figures 3–5.

Discussion

Antiscatter grid (ASG) removal results in significantly lower radiation dose to patients during cardiologic and pediatric interventional procedures (6–15). We investigated the hypothesis that such a technique could be applied to decrease radiation dose to adults undergoing digital subtraction angiography (DSA) while maintaining acceptable diagnostic image quality. We found that *(a)* ASG removal reduced the mean dose per angiographic sequence by approximately 30% (mean dose-area product [DAP] without and with ASG, 135.6 and 202 μGy/m^2, respectively; mean air kerma without and with ASG, 24 and 35.3, respectively; $P < .001$) independently of body mass index [BMI] ($P < .001$) and *(b)* images without ASG maintained diagnostic quality in the independent and blinded evaluation of experienced neurointerventionalists.

Dose-reducing techniques are critical during spinal DSA considering the many vessels DSA is used to investigate. Our study shows that gridless spinal DSA reduced exposure by approximately 30%, regardless of body habitus, while preserving its diagnostic value. Readers classified all images as diagnostic (of good or moderate quality): As expected, images obtained without ASG were classified as being of moderate quality more often than their counterparts obtained with ASG. Although gridless angiographic imaging is noisier as a result of the increased x-ray scatter, two experienced angiographers could not consistently determine which protocol had been used when images were reviewed separately. The decrease in image quality is thus insufficient to categorize an individual image as a grid-in or grid-out image.

Gridless angiography is an established dose-reduction tool applied notably in pediatric angiography and, more recently, interventional cardiology and temporal bone imaging. Most studies on dose reduction and image quality were performed with phantoms or animal models or were retrospective reviews of patient series (6,10–18). The 30% dose reduction observed in our study, which to our knowledge is the only prospective evaluation of gridless angiography comparing images obtained in direct succession and varying only by the presence of ASGs, is consistent with the findings from these earlier investigations (9,10,12,19).

Table 2: Dose Reduction in Spinal DSA with and without Antiscatter Grids

Variable	Air Kerma at Reference Point (mGy)			Dose-Area Product (μGy/m²)		
	Grid-in	Grid-out	*P* Value	Grid-in	Grid-out	*P* Value
All participants (*n* = 53)	35.3 ± 13.7 (14–68.2)	24.0 ± 10.6 (8.3–48.1)	<.001	202 ± 100.2 (38.6–548.5)	135.6 ± 68.5 (31.5–319.6)	<.001
Low BMI (≤25 kg/m²) group (*n* = 20)	28.5 ± 11.4 (14–55.8)	18.3 ± 10.7 (8.3–48.1)	<.001	151.9 ± 64.9 (38.6–310)	93.1 ± 48.9 (31.5–211.5)	<.001
High BMI (>25 kg/m²) group (*n* = 33)	39.9 ± 13.3 (21.4–68.2)	27.5 ± 8.8 (11–46.7)	<.001	232.3 ± 105.5 (77.4–548.5)	161.4 ± 64.4 (55.6–319.6)	<.001

Note.—Data are means ± standard deviations, with ranges in parentheses. Dose references are per key angiographic run (ie, significant run showing either the artery of Adamkiewicz or the abnormality). BMI = body mass index.

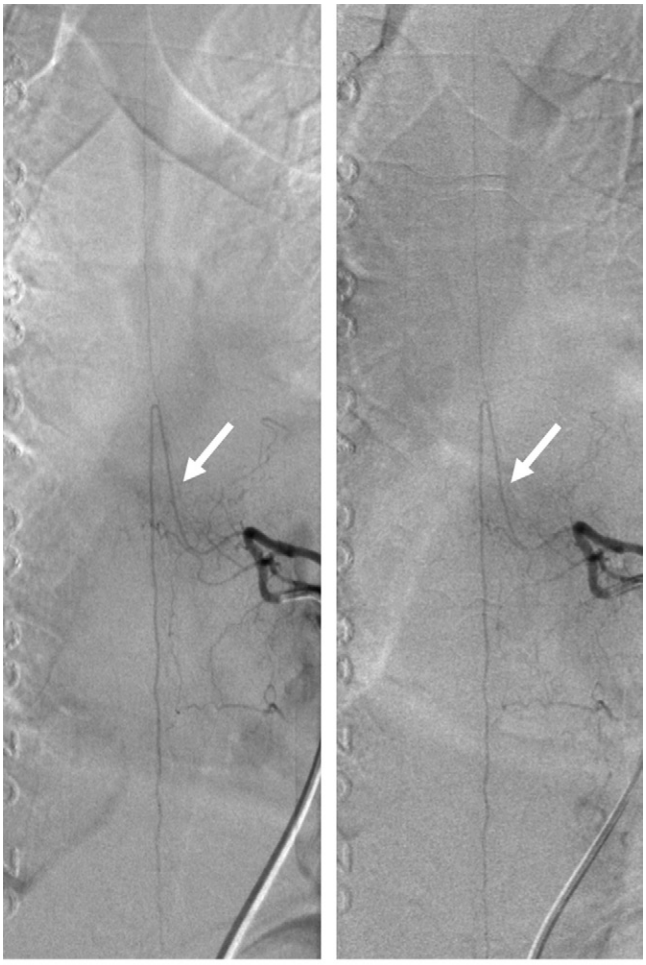

a. b.

Figure 3: Spinal digital subtraction angiograms in a 21-year-old man with a cord hemorrhage. Injection of the left T9 intersegmental artery (posteroanterior projection) shows a normal artery of Adamkiewicz (arrow) **(a)** with and **(b)** without antiscatter grids. Grid removal reduced both air kerma and dose-area product from 26 mGy and 116 μGy/m² to 18 mGy and 82 μGy/m² (30% and 29% reduction), respectively.

Partridge et al (10) assessed coronary angiography performed without ASGs and noted mean DAP reductions of 39% and 23% during diagnostic and interventional procedures, respectively, without a substantial decrease in image quality. They concluded that ASG removal should be implemented in both adult and pediatric interventional cardiology. A recent study considering cardiac catheterization with and without ASGs in a phantom and in patients with BMI lower than 25 kg/m² showed a dose reduction of up to 46.6% in patients, without substantial decrease in image quality, and a dose reduction of 70% in phantoms, with a more prominent decrease in image quality in large phantoms (20). In their evaluation of gridless electrophysiology procedures, Smith et al (21) observed unchanged procedural outcomes despite a perceptible decrease in image quality. Gridless angiography is now advocated for all pediatric interventional radiology and cardiology procedures (18,22). It is, in our opinion, mandatory for most pediatric diagnostic neuroangiographic examinations and may be applied to selected adult cranial procedures with similar dose-reduction benefits (15).

ASG removal does not affect the angiographic workflow and decreases the dose regardless of other settings, including frame rates, magnification, and geometric factors. It can be combined with other dose reduction strategies, such as variable frame rate and low dose-per-frame protocols, to optimize radiation management. On modern equipment, ASGs can be removed or reinserted in a matter of seconds, allowing quick repositioning for a specific component of a procedure (23). During spinal DSA, for example, ASGs may be necessary only for the abdominal portion of the study.

Spinal DSA addresses some of the smallest vessels subjected to angiographic evaluation. The artery of Adamkiewicz has a mean diameter of 1.8 mm; the radiculomeningeal arteries feeding spinal arteriovenous fistulas are typically inframillimetric (24). In contrast, the mean arterial diameter of the celiac, splenic, and left gastric arteries is about 8, 6, and 4 mm, respectively (25); the diameter of normal pediatric coronary arteries ranges between 2 and 5 mm (26). Spinal DSA involves the same body regions as interventions in the chest, abdomen, or pelvis. ASG removal should thus be effective in a wide range of diagnostic and interventional procedures. In a recent study of the benefits of grid removal on routine biliary interventions, Cortis et al (27) noted a 39% dose reduction, with no effect on procedural duration and outcomes. They emphasized the importance of dose optimization during interventions frequently repeated in the same patient. Future studies investigating the quality of images obtained without

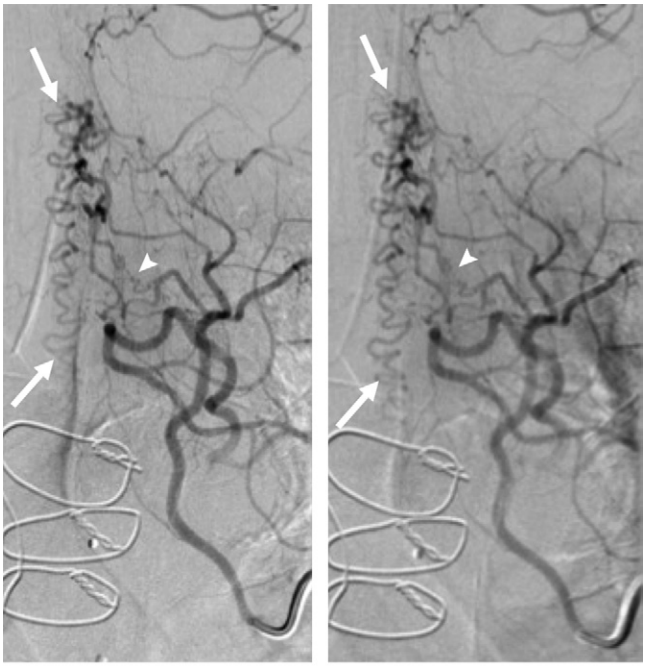

a. b.

Figure 4: Spinal digital subtraction angiograms in a 65-year-old man with progressive myelopathy. Injection of the left T3 intersegmental artery shows small radiculomeningeal arteries supplying a spinal dural arteriovenous fistula (arrowhead) as well as the dilated and serpiginous perimedullary draining veins (arrows) **(a)** with and **(b)** without antiscatter grids. The feeding arteries and draining veins are well appreciated in both injections. Antiscatter grid removal reduced both air kerma and dose-area product from 49 mGy and 315 μGy/m^2 to 33 mGy and 210 μGy/m^2, respectively (33% reduction for both).

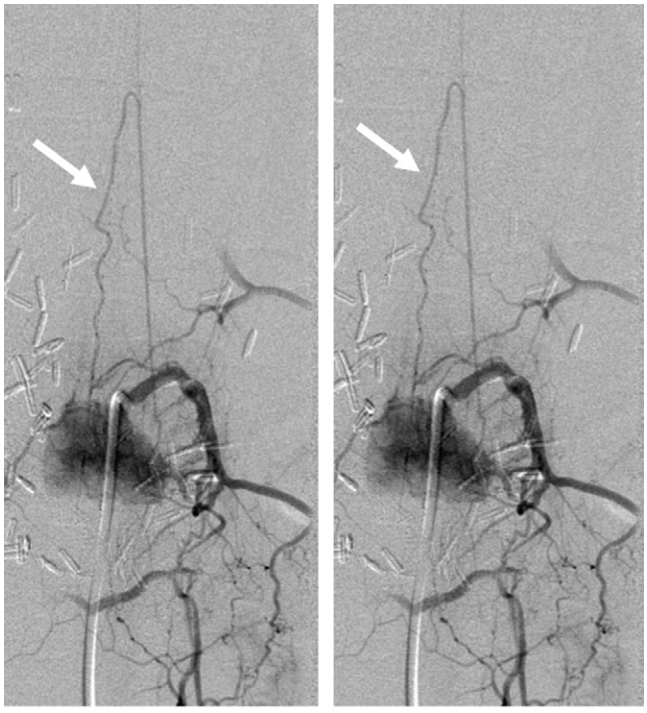

a. b.

Figure 5: Spinal digital subtraction angiograms in a 52-year-old man with a hypervascular vertebral metastasis. Injection of the left T12 intersegmental artery shows tumoral blush and the artery of Adamkiewicz (arrow) **(a)** with and **(b)** without antiscatter grids. The tumoral blush and the radiculomedullary artery arising from the intersegmental artery supplying the tumor are clearly appreciated in both injections. Antiscatter grid removal reduced both air kerma and dose-area product from 60 mGy and 457 μGy/m^2 to 32 mGy and 249 μGy/m^2, respectively (46% reduction for both).

ASGs during thoracic, abdominal, and pelvic procedures should help widen the scope of this simple dose-reduction technique.

Our study had limitations. Contrast material injections for all test acquisitions were performed by hand (by one operator who was not blinded to the acquisition type), and although extreme attention was paid to keep the volume and injection pressure identical (as can be observed in the consistent degree of opacification of studied structures in images with and those without ASG), this mode of administration is not as reproducible as automatic pump injection. Hand injections were still preferred because they are considered safer in our practice. Furthermore, all injections being performed by the same operator could limit generalizability. The patient-to-detector distance, which plays a role in the attenuation of scattered radiation, was not recorded; this factor is mitigated by our routine practice of keeping the patient-to-detector distance as short as possible and by the fact that the detector was not moved between the two test acquisitions. We acknowledge that subjective image quality is a weaker measure than diagnostic accuracy. Nevertheless, correct categorization of findings independently of grid status indirectly demonstrates acceptable accuracy irrespective of the presence of the grid. For practical purposes, we decided to provide readers with 40 images from 20 participants. Although selection bias was avoided by randomly choosing images from 10 participants in the "no abnormality" group and 10 participants in the "abnormality" group, the images do not represent our entire sample. Although care was taken to provide readers with representative images at the time of maximum opacification of the key finding, readers were not given the entire dynamic DSA acquisition. This limited the evaluation to a portion of the study angiogram. Finally, our study exclusively addresses radiation produced during DSA acquisitions, not during pulsed fluoroscopy. However, it can be assumed that gridless fluoroscopy offers benefits akin to those of gridless angiography, as suggested in prior studies (6,17).

Radiation protection strategies, in agreement with the "as low as reasonably achievable" principle, should help angiographers aim for diagnostic value over aesthetic satisfaction (16,28–34). Our study shows that antiscatter grid removal during spinal digital subtraction angiography depicts subtle vascular structures with a mean dose reduction of 30%, without significant loss of image quality, irrespective of participants' body mass index. In the future, gridless angiography may also have broader applications, notably regarding diagnostic and interventional procedures involving the chest, abdomen, and pelvis.

Author contributions: Guarantors of integrity of entire study, E.O., A.E.M., M.S.P., P.G.; study concepts/study design or data acquisition or data analysis/interpretation, all authors; manuscript drafting or manuscript revision for important intellectual content, all authors; approval of final version of submitted manuscript,

all authors; agrees to ensure any questions related to the work are appropriately resolved, all authors; literature research, E.O., A.E.M., P.G.; clinical studies, E.O., A.E.M., M.S.P., P.G.; statistical analysis, E.O., A.E.M.; and manuscript editing, E.O., A.E.M., M.S.P., P.G.

Disclosures of Conflicts of Interest: E.O. disclosed no relevant relationships. **A.E.M.** disclosed no relevant relationships. **D.S.M.** disclosed no relevant relationships. **M.S.P.** disclosed no relevant relationships. **P.G.** Activities related to the present article: institution received a grant from Siemens Medical. Activities not related to the present article: is a consultant for Cerenovus. Other relationships: has a patent issued to Artventive.

References

1. Chen J, Gailloud P. Safety of spinal angiography: complication rate analysis in 302 diagnostic angiograms. Neurology 2011;77(13):1235–1240.
2. Krings T, Lasjaunias PL, Hans FJ, et al. Imaging in spinal vascular disease. Neuroimaging Clin N Am 2007;17(1):57–72.
3. Eddleman CS, Jeong H, Cashen TA, et al. Advanced noninvasive imaging of spinal vascular malformations. Neurosurg Focus 2009;26(1):E9.
4. Sharma AK, Westesson PL. Preoperative evaluation of spinal vascular malformation by MR angiography: how reliable is the technique: case report and review of literature. Clin Neurol Neurosurg 2008;110(5):521–524.
5. Di Chiro G, Wener L. Angiography of the spinal cord. A review of contemporary techniques and applications. J Neurosurg 1973;39(1):1–29.
6. Drury P, Robinson A. Fluoroscopy without the grid: a method of reducing the radiation dose. Br J Radiol 1980;53(626):93–99.
7. Wagner LK, Eifel PJ, Geise RA. Potential biological effects following high X-ray dose interventional procedures. J Vasc Interv Radiol 1994;5(1):71–84.
8. Neitzel U. Grids or air gaps for scatter reduction in digital radiography: a model calculation. Med Phys 1992;19(2):475–481.
9. Söderman M, Hansson B, Axelsson B. Radiation dose and image quality in neuroangiography: effects of increased tube voltage, added x-ray filtration and antiscatter grid removal. Interv Neuroradiol 1998;4(3):199–207.
10. Partridge J, McGahan G, Causton S, et al. Radiation dose reduction without compromise of image quality in cardiac angiography and intervention with the use of a flat panel detector without an antiscatter grid. Heart 2006;92(4):507–510.
11. Strauss KJ, Racadio JM, Abruzzo TA, et al. Comparison of pediatric radiation dose and vessel visibility on angiographic systems using piglets as a surrogate: antiscatter grid removal vs. lower detector air kerma settings with a grid - a preclinical investigation. J Appl Clin Med Phys 2015;16(5):408–417.
12. McFadden SL, Hughes CM, Mooney RB, Winder RJ. An analysis of radiation dose reduction in paediatric interventional cardiology by altering frame rate and use of the anti-scatter grid. J Radiol Prot 2013;33(2):433–443.
13. Mekabaty AE, Pross SE, Martinez M, Carey JP, Pearl MS. Reducing radiation dose for high-resolution flat-panel CT imaging of superior semicircular canal dehiscence. Otol Neurotol 2018;39(8):e683–e690.
14. Onnasch DG, Schemm A, Kramer HH. Optimization of radiographic parameters for paediatric cardiac angiography. Br J Radiol 2004;77(918):479–487.
15. Morris PP, Geer CP, Singh J, Brinjikji W, Carter RE. Radiation dose reduction during neuroendovascular procedures. J Neurointerv Surg 2018;10(5):481–486.
16. Pearl MS, Torok CM, Messina SA, et al. Reducing radiation dose while maintaining diagnostic image quality of cerebral three-dimensional digital subtraction angiography: an in vivo study in swine. J Neurointerv Surg 2014;6(9):672–676.
17. Gray JE, Swee RG. The elimination of grids during intensified fluoroscopy and photofluoro spot imaging. Radiology 1982;144(2):426–429.
18. Ubeda C, Vano E, Gonzalez L, Miranda P. Influence of the antiscatter grid on dose and image quality in pediatric interventional cardiology X-ray systems. Catheter Cardiovasc Interv 2013;82(1):51–57.
19. King JM, Elbakri IA, Reed M. Antiscatter grid use in pediatric digital tomosynthesis imaging. J Appl Clin Med Phys 2011;12(4):3641.
20. Roy JR, Sun P, Ison G, et al. Selective anti-scatter grid removal during coronary angiography and PCI: a simple and safe technique for radiation reduction. Int J Cardiovasc Imaging 2017;33(6):771–778.
21. Smith IR, Stafford WJ, Hayes JR, Adsett MC, Dauber KM, Rivers JT. Radiation risk reduction in cardiac electrophysiology through use of a gridless imaging technique. Europace 2016;18(1):121–130.
22. Hill KD, Frush DP, Han BK, et al. Radiation safety in children with congenital and acquired heart disease: a scientific position statement on multimodality dose optimization from the image gently alliance. JACC Cardiovasc Imaging 2017;10(7):797–818.
23. Roy J, Weaver J, Sader M, Ison G. Removing the antiscatter grid: a simple way to lower radiation during both angiography and PCI. Heart Lung Circ 2015;24(Supplement 3):S298.
24. Boll DT, Bulow H, Blackham KA, Aschoff AJ, Schmitz BL. MDCT angiography of the spinal vasculature and the artery of Adamkiewicz. AJR Am J Roentgenol 2006;187(4):1054–1060.
25. Malnar D, Klasan GS, Miletić D, et al. Properties of the celiac trunk--anatomical study. Coll Antropol 2010;34(3):917–921.
26. Arjunan K, Daniels SR, Meyer RA, Schwartz DC, Barron H, Kaplan S. Coronary artery caliber in normal children and patients with Kawasaki disease but without aneurysms: an echocardiographic and angiographic study. J Am Coll Cardiol 1986;8(5):1119–1124.
27. Cortis K, Miraglia R, Maruzzelli L, Gerasia R, Tafaro C, Luca A. Removal of the antiscatter grid during routine biliary interventional procedures performed in a flat-panel interventional suite: preliminary data on image quality and patient radiation exposure. Cardiovasc Intervent Radiol 2014;37(4):1078–1082.
28. The 2007 recommendations of the International Commission on Radiological Protection. ICRP publication 103. Ann ICRP 2007;37(2-4):1–332.
29. Schneider T, Wyse E, Pearl MS. Analysis of radiation doses incurred during diagnostic cerebral angiography after the implementation of dose reduction strategies. J Neurointerv Surg 2017;9(4):384–388.
30. Kahn EN, Gemmete JJ, Chaudhary N, et al. Radiation dose reduction during neurointerventional procedures by modification of default settings on biplane angiography equipment. J Neurointerv Surg 2016;8(8):819–823.
31. Pearl MS, Torok C, Wang J, Wyse E, Mahesh M, Gailloud P. Practical techniques for reducing radiation exposure during cerebral angiography procedures. J Neurointerv Surg 2015;7(2):141–145.
32. Söderman M, Holmin S, Andersson T, Palmgren C, Babic D, Hoornaert B. Image noise reduction algorithm for digital subtraction angiography: clinical results. Radiology 2013;269(2):553–560.
33. Honarmand AR, Shaibani A, Pashaee T, et al. Subjective and objective evaluation of image quality in biplane cerebral digital subtraction angiography following significant acquisition dose reduction in a clinical setting. J Neurointerv Surg 2017;9(3):297–301.
34. Yi HJ, Sung JH, Lee DH, Kim SW, Lee SW. Analysis of radiation doses and dose reduction strategies during cerebral digital subtraction angiography. World Neurosurg 2017;100:216–223.